Rheology of Miscible Blends: SAN and PMMA†

Jai A. Pathak

Department of Chemical Engineering, The Pennsylvania State University, University Park, Pennsylvania 16802-4400

Ralph H. Colby,* Sudesh Y. Kamath, and Sanat K. Kumar

Department of Materials Science and Engineering, The Pennsylvania State University, University Park, Pennsylvania 16802-5007

Reimund Stadler‡

Makromolekulare Chemie II, Universität Bayreuth, Bayreuth, Germany 95440

Received April 13, 1998; Revised Manuscript Received September 14, 1998

ABSTRACT: The linear viscoelasticity of miscible blends of a random copolymer of 80% styrene and 20% acrylonitrile and poly(methyl methacrylate) has been investigated using oscillatory shear. The Flory−Huggins interaction parameter of this blend is weakly negative. The glass transitions of the pure components are very close ($\Delta T_g = 20$ K). The blends are *thermorheologically simple*, in that the oscillatory shear response at different temperatures can be superimposed with the empirical time−temperature superposition principle with a precision similar to that for the pure component polymers. These results are anticipated by a theory of concentration-fluctuation-induced dynamic heterogeneities in miscible polymer blends. While sizable concentration fluctuations are present in this blend system, they do not complicate the dynamics, because all compositions have similar local dynamics. We suggest a simple phase diagram based on this model, that should be useful for deciding whether time−temperature superposition will be valid for a given blend with weak energetic interactions. Regions of thermorheological complexity are separated from regions of thermorheological simplicity on a plot of the range of blend free volume studied against the glass transition contrast of the components (ΔT_g).

I. Introduction

Miscible polymer blends have recently seen a tremendous surge in industrial applications[1,2] because they offer an inexpensive route to new polymeric materials. For example, the scope of practical applications of an amorphous polymer can be increased by blending it with a polymer of higher T_g. However, there is no reliable method of predicting the viscosity of miscible blends. Empirical relations[2] for the composition dependence of viscosity are kept too general to have any predictive capabilities.

One complication in miscible blends is that the empirical time−temperature superposition (tTS) principle[3] breaks down in some systems.[4−13] On the other hand, some miscible blends are thermorheologically simple.[14,15] Before we can develop a model to predict their viscosity, it is imperative to study the rheology of miscible blends, in order to get a fundamental understanding of the physical principles which control blend dynamics.

We report linear viscoelastic data on miscible blends of a random copolymer of styrene and acrylonitrile (SAN) and poly(methyl methacrylate) (PMMA). This blend is characterized by *dynamic symmetry*; that is, the two pure components have closely-matched glass transition temperatures ($\Delta T_g = 20$ K) and even more closely-matched Vogel temperatures ($\Delta T_\infty \leq 5$ K). The linear viscoelastic responses of PMMA, SAN, and several blends have been investigated by means of oscillatory shear and found to obey tTS reasonably well. We explain why tTS works for such dynamically symmetric blends and give specific criteria for expecting thermorheological complexity, based on a simple composition fluctuation model.[16,17]

II. Background

A. Thermodynamics. It is well-known that mixtures of SAN and PMMA can be miscible.[1,18] The phase behavior of SAN/PMMA blends is a function of the microstructural details of each polymer: the acrylonitrile (AN) content of the SAN[1,18−22] and the tacticity of the PMMA.[23] According to Paul *et al.*,[24] miscibility is observed in these blends for SAN with a AN content between approximately 9% and 33% by weight. Syndiotactic PMMA (s-PMMA) is found to be most miscible with SAN of various AN contents, followed by heterotactic PMMA (h-PMMA) and isotactic PMMA (i-PMMA), respectively. In this study we use PMMA that is 80% syndiotactic and 20% heterotactic, and SAN containing 20% acrylonitrile and 80% styrene.

Since this blend is characterized by closely-matched glass transition temperatures ($T_g^{PMMA} = 130$ °C and $T_g^{SAN} = 110$ °C), measurement of the T_g of the blend by DSC does not provide information about miscibility. In miscible blends, the glass transition is known to broaden significantly, especially with increasing concentration of the component with the higher T_g.[5,25] Hourtston *et al.*[26] have used modulated DSC to study the thermal behavior of SAN/PMMA blends. One clear peak is seen in the curve of dC_p/dT versus temperature, strongly suggesting that the blend is miscible. The most convincing evidence for mixing on a segmental level comes from

† We dedicate this paper to the memory of Reimund Stadler, with whom we wrote the paper.

‡ Deceased.

10.1021/ma9805708 CCC: $15.00
Published on Web 12/01/1998

cross-polarization magic angle spinning (CPMAS) ^{13}C NMR experiments.[27] The spin−lattice relaxation times of carbon atoms (T_1) move closer together in blends than they are in the pure components of SAN and PMMA, and the CPMAS resonance intensity decays are exponential for the blends.

The exact physical principles which drive miscibility in SAN/PMMA blends have been debated. It is known that PMMA is miscible neither with polystyrene nor with polyacrylonitrile.[1] Some workers[24,28] are of the viewpoint that miscibility in this blend is due to the strong repulsive interactions between S and AN segments of the copolymer. Even though there is no favorable binary interaction either between the MMA and S segments or between the MMA and AN segments, this blend has been documented to have a favorable negative enthalpy of mixing.[28] However, ^{13}C NMR suggests[37] that the intermolecular charge-transfer interaction between SAN and PMMA is responsible for miscibility. Feng *et al.*[27] reject the rationalization of the miscibility in this blend in terms of the so-called repulsion model,[28,29] since the results of their NMR experiments show a specific interaction between the phenyl groups of the SAN and the carbonyl group on the PMMA.

Small-angle neutron scattering, done by Kirste and co-workers,[30−32] has been used to determine $\chi \gtrsim -0.01$, which depends somewhat on the temperature, the chain length of the components, and the blend composition. This χ value puts SAN/PMMA in the class of weakly interacting blends, where concentration fluctuations are important. For blends in this class, where χ is not too strongly negative, our concentration fluctuation model predicts that the precise value of χ plays a very minor role in blend dynamics.[33]

B. Dynamics. Kim *et al.*[34,35] have used forward recoil spectrometry to determine the tracer diffusion coefficients of deuterated PMMA and deuterated SAN in SAN/PMMA blends. They report that SAN and PMMA show identical temperature dependences for their diffusion coefficients in SAN/PMMA blends, in the range $40\ K < T - T_g < 100\ K$. Therefore, we know that the blends are thermorheologically simple far above T_g, and we now extend measurements closer to the glass transition using oscillatory shear. Oultache *et al.*[36] have used infrared dichroism to study orientation relaxation in uniaxially stretched films of SAN/PMMA blends slightly above their glass transition ($3\ K < T - T_g < 21\ K$). PMMA is observed to have oriented more than SAN in any blend at a given stretching rate. PMMA also relaxes its orientation during the stretch faster than SAN does, as shown by experiments performed using different stretching rates. These results suggest that SAN and PMMA may have different segmental dynamics close to T_g.

The linear viscoelasticity of SAN/PMMA blends has been reported previously. Wu[37] has reported the zero shear viscosity (η_0) and found a monotonic dependence on blend composition. In another study, Wu[38] has reported results on oscillatory shear and creep experiments on SAN/PMMA blends, where he finds that the tTS works well in the temperature range $20\ K < T - T_g < 80\ K$. Han and Kim[39−41] have reported that plots of G' versus G'' for SAN/PMMA blend data taken in the temperature interval $40\ K < T - T_g < 110\ K$ result in temperature-independent curves, suggesting that tTS should apply.

Table 1. Molecular Weights

	M_w	M_w/M_n
PMMA	296 000	1.1
SAN1	80 000	1.3
SAN2	243 000	1.5

Table 2. Thermorheological Characteristics

polymer	T_g (°C)	C_1^g	T_∞ (°C)	$10^4\alpha_f$ (K^{-1})
PMMA	130	11.2	70	6.5
SAN1	110	10.6	70	10.
SAN2	110	10.0	70	11.
20 wt % SAN1/ 80 wt % PMMA	120	11.7	70	7.4
30 wt % SAN1/ 70 wt % PMMA	118	11.8	70	7.7
40 wt % SAN2/ 60 wt % PMMA	117	10.2	70	9.1

III. Experimental Section

A. Materials, Characterization, and Blend Preparation. A random copolymer of 20% acrylonitrile and 80% styrene (SAN) was obtained from BASF, with $M_w = 75\ 000$ and $M_w/M_n = 2.4$. The copolymer composition is near the azeotropic composition (25% AN), and its composition is kept uniform throughout the polymerization by appropriate addition of AN. Elemental analysis indicated the copolymer is (19 ± 2)% AN. The fact that moldings of this SAN were highly transparent indicates that there are no large heterogeneities in composition, since mixtures of SAN copolymers with compositions differing by 4−6% are turbid due to immiscibility. This commercial SAN was fractionated using toluene and petroleum ether.

The PMMA was prepared by anionic polymerization in THF at −90 °C with a diphenyl hexyl lithium initiator. ^1H NMR was used to determine the sequence distribution of the PMMA: 80% of the triads were syndiotactic, and 20% were heterotactic. The weight-average molecular weights (M_w) of the two SAN fractions and the PMMA are listed in Table 1, along with their polydispersities (M_w/M_n). These quantities were determined by size-exclusion chromatography with refractive index and viscosity detectors utilizing universal calibration with polystyrene standards.

A blend consisting of 20 wt % SAN1 and 80 wt % PMMA was prepared as follows. A 1 wt % solution of the polymers in tetrahydrofuran was added dropwise to an excess volume (about 20 times) of methanol (nonsolvent). The resulting stringy white precipitate was filtered and then dried in a vacuum oven, first at 50 °C and then at 70 °C. The blend was dried to constant mass under vacuum in roughly 4 weeks. Blends of 30 wt % SAN1/70 wt % PMMA and 40 wt % SAN2/60 wt % PMMA were also prepared by a similar procedure.

The glass transition temperatures of the pure polymers and their blends, determined by differential scanning calorimetry on a Seiko Instruments SSC 5200 DSC with 5−10 mg of sample, are listed in Table 2. Heating and cooling rates of 10 K/min were consistently used, and the reported T_g was taken as the midpoint of the second heating of each sample. The DSC was calibrated with an indium standard, which melts at 156.6 °C. We used optical microscopy to estimate the cloud points of two of our blends. The 20% SAN blend had a cloud point of 230 °C, while the 30% SAN blend had a cloud point of 240 °C, which are well in excess of our experimental temperatures and consistent with previous reports for SAN/PMMA blends of similar molecular weight.[22,24] SAN/PMMA blends generally exhibit a well-defined lower critical solution temperature,[42−44] consistent with the SANS observation that χ increases with temperature.[30−32]

B. Rheology. Oscillatory shear rheometry was performed on all three blends and the pure components, after molding in a vacuum-assisted compression mold 50 K above T_g, using a Rheometric Scientific ARES rheometer with a force-rebalance transducer. The applied strain amplitudes ($0.001 < \gamma_0 < 0.1$) were always less than the maximum limiting strain for

producing a linear viscoelastic response, as determined by strain sweep experiments at various frequencies. For experiments at temperatures higher than $T_g + 30$ K, 25 mm diameter parallel plates were used. For experiments between T_g and $T_g + 30$ K, 7.9 mm diameter parallel plates were used to reduce the influence of transducer compliance. Temperature control during the experiments was maintained by a steady flow of heated nitrogen gas through the sample chamber. Frequencies between 10^{-2} and 10^2 rad/s were typically used, although slightly lower frequencies (of order 10^{-3} rad/s) were used in some experiments to measure the viscoelastic response on longer time scales. The data presented here are not corrected for transducer compliance effects, which affect the data in the 7.9 mm diameter plates when the complex modulus exceeds 10^9 dyn/cm^2. Transducer compliance only lowers the moduli slightly at the highest frequencies near T_g (in Figures 1c and 2).

As a final note about experimental details, it must be mentioned that solvents such as THF and water, which are capable of hydrogen bonding with PMMA, cannot be completely removed from PMMA, even under vacuum at temperatures close to T_g. This poses a problem during experiments, because the solvent forms bubbles at elevated temperatures. For quantitative viscoelastic data, the sample must be kept free of voids. To accomplish this, each sample was first molded in a vacuum-assisted compression mold to produce a bubble-free disk. This sample was heated to a temperature slightly above the highest planned temperature of measurement. Sufficient time (typically, about 8−12 h) was provided for the sample to equilibrate under nitrogen at this elevated temperature. After the sample had finished bubbling, it was remolded, yielding a disk that remained bubble-free at all measurement temperatures. We always rerun the first temperature of measurement after completing the final temperature of measurement with each blend, to check that no changes have occurred in our blends in the rheometer.

IV. Results

The tTS principle[3] relates the frequency ω dependence of the complex modulus G^* at any temperature T to that at any reference temperature, which we take to be the glass transition temperature, T_g.

$$G^*(\omega;T) = b_T G^*(a_T\omega;\, T_g) \qquad (1)$$

A single frequency-scale shift factor a_T and a single modulus-scale shift factor b_T allow us to superimpose all frequency-dependent data at temperature T with data at the reference temperature T_g. This simple empirical scheme, based on the notion that all polymeric relaxations derive from the same fundamental segmental motions, allows the construction of master curves of rheological functions (such as G^*) that span many orders of magnitude in time or frequency and are simply not otherwise attainable. As such, this principle is used pervasively in the rheological literature.[3] Our materials showed small modulus-scale shifts ($b_T \cong 1$) that we do not discuss here and comparatively large frequency-scale shifts (discussed below) which follow the WLF equation.

Time−temperature superposition was applied to each of the pure components, and master curves were prepared according to this principle. The master curve for PMMA is shown in Figure 1a, and the master curves for the two fractions of SAN are presented in Figure 1b and c.

Time−temperature superposition was also applied to the blends. The master curves for the dynamic storage and loss moduli and the loss tangent of the 20 wt % SAN1/80 wt % PMMA blend, the 30 wt % SAN1/70 wt % PMMA blend, and the 40 wt % SAN2/60 wt % PMMA blend are given in parts a, b, and c of Figure 2, respectively.[60]

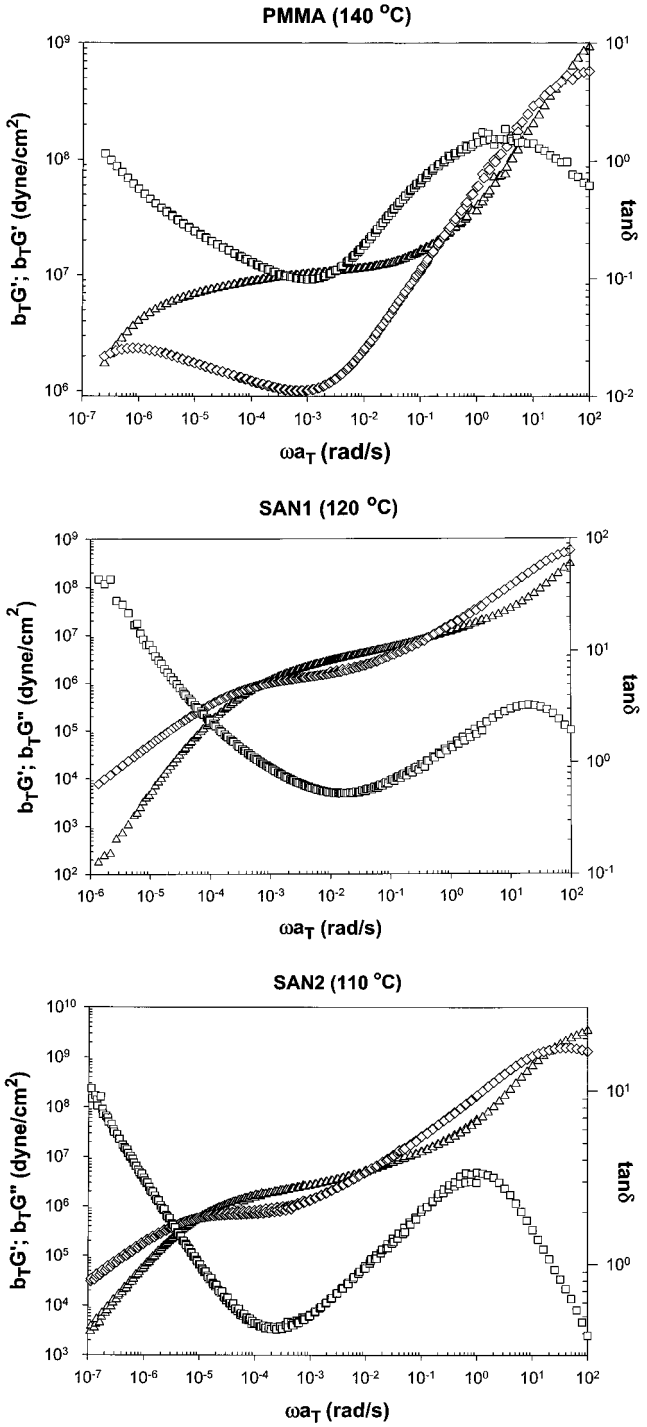

Figure 1. Master curves of the storage modulus (G', triangles), loss modulus (G'', diamonds), and loss tangent (tan δ, squares) for the pure components: (a, top) PMMA referenced to 140 °C ($=T_g + 10$ K) using data at 140, 150, 160, 170, 180, 185 °C; (b, middle) SAN1 referenced to 120 °C ($=T_g + 10$ K) using data at 120, 130, 140, 150, 160 °C; (c, bottom) SAN2 referenced to 110 °C ($=T_g$) using data at 110, 120, 130, 140, 150, 160, 170 °C.

To ensure that modulus-scale shifts do not allow false superposition, we make extensive use of the loss tangent.

$$\tan\delta = \frac{G''}{G'} \qquad (2)$$

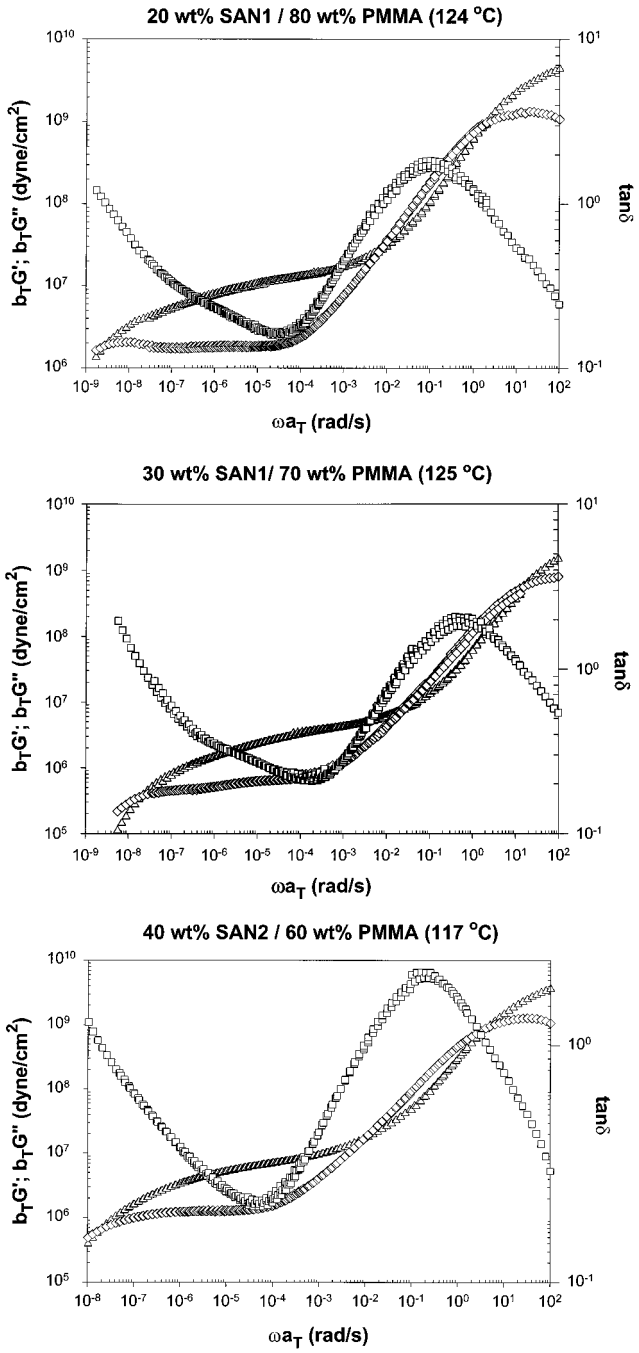

Figure 2. Master curves of the storage modulus (G', triangles), loss modulus (G'', diamonds), and loss tangent (tan δ, squares) for the blends: (a, top) 20 wt % SAN1/80 wt % PMMA referenced to 124 °C ($=T_g + 4$ K) using data at 124, 129, 134, 144, 154, 164, 174, 179, 184 °C; (b, middle) 30 wt % SAN1/70 wt % PMMA referenced to 125 °C ($=T_g + 7$ K) using data at 125, 130, 140, 146.5, 154.4, 166.2, 185.4, 204.4, 223 °C; (c, bottom) 40 wt % SAN2/60 wt % PMMA referenced to 117 °C ($=T_g$) using data at 117, 127, 137, 147, 157, 167 °C.

Since the loss tangent is given by the ratio of G'' and G', any modulus-scale shift factors used will be automatically canceled. Thus, when a master curve for tan δ is constructed, the effectiveness of the frequency-scale shift factor (a_T) alone can be unambiguously investigated. The frequency-scale shift a_T is, therefore, determined by shifting tan δ, and b_T is subsequently determined from the modulus scale shift of $G^*(a_T\omega; T_g)$ required to obtain superposition of the complex modulus. We notice from Figures 1 and 2 that the quality of the superposition is only slightly worse for the blends than for the pure components. However, it is imperfect in all cases, as has been previously reported by Plazek for many polymers near their glass transition.[45−47]

The temperature dependence of the frequency-scale shift factor a_T, required to shift data from T to T_g, is empirically described by the WLF equation.[3,48]

$$\log a_T = -C_1^g \left[\frac{T - T_g}{T - T_\infty}\right] \tag{3}$$

C_1^g is a WLF constant referenced to the glass transition temperature (T_g), and T_∞ is the Vogel temperature (where the viscosity diverges). Note that, in the WLF work,[3,48] a second constant C_2^g was also used, with $C_2^g = T_g - T_\infty$. Equation 3 is precisely the form proposed by Vogel in 1921.[49] Plazek has noted that the preferred procedure to evaluate WLF coefficients is to plot log a_T versus $(T - T_g)/(T - T_\infty)$ (based on eq 3) using the Vogel temperature T_∞ as a free parameter to linearize the plot.[45] Provided that data are taken both close to T_g and over a sufficiently wide range, this procedure determines the Vogel temperature to within ±2 K. Of the many procedures suggested to determine WLF coefficients,[3] we find this procedure to be the most objective and reliable, and hence we utilize it exclusively.

In the free volume model,[3] the frequency-scale shift factor is related to the fractional free volume f and its value f_g at the glass transition T_g.

$$a_T = \exp\left[B\left(\frac{1}{f} - \frac{1}{f_g}\right)\right] \tag{4}$$

B is a dimensionless material-specific parameter of order 1. To relate this to the WLF equation (eq 3), the free volume is assumed to be a linear function of temperature, and the coefficient of thermal expansion of the free volume (α_f) can then be calculated from the WLF constants.[3]

$$\alpha_f = \frac{B}{C_1^g (T_g - T_\infty) \ln 10} \tag{5}$$

Vogel plots (log a_T versus $(T - T_g)/(T - T_\infty)$ based on eq 3) for the blends and the pure components were prepared by adjusting T_∞ to obtain linearity. Adjustments of ±3 K lead to detectable departures from linearity, and we find that, for all blends and pure components, $T_\infty = 70 \pm 3$ K. The Vogel plots with $T_\infty = 70$ K are shown in Figure 3a, from which C_1^g is determined from the slope. These coefficients, as well as the coefficients of thermal expansion of the free volume α_f (calculated from eq 5 assuming the constant $B = 1$), are tabulated for the blends and their pure components in Table 2. The differences in C_1^g and α_f observed for SAN1 and SAN2 are beyond the experimental uncertainty, assuming the Vogel temperatures are identical. This probably indicates slight microstructural differences between these fractions; the smaller C_1^g is also seen in the blend (see Table 2 and Figure 3a). The Vogel temperatures of PMMA and SAN are the same within experimental error ($\Delta T_\infty \leq 5$ K) and considerably smaller than the difference between their glass transition temperatures ($\Delta T_g = 20$ K).

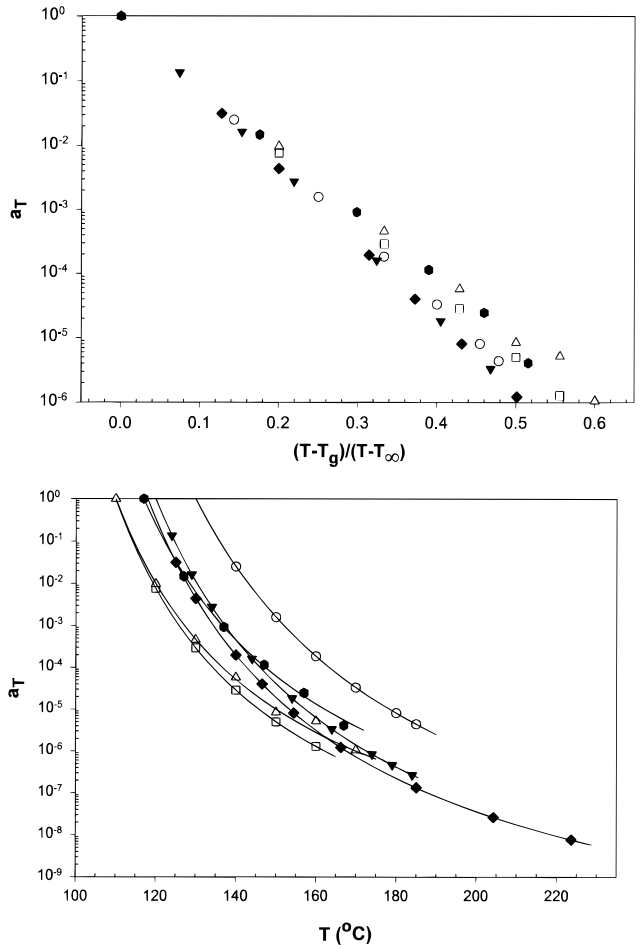

Figure 3. Temperature dependence of the frequency-scale shift factor a_T (a, top) in the form of a Vogel plot (eq 3) with $T_\infty = 70$ °C and (b, bottom) as a function of temperature, for PMMA (open circles), SAN1 (open squares), SAN2 (open triangles), and their blends: 20 wt % SAN1/80 wt % PMMA (filled inverted triangles), 30 wt % SAN1/70 wt % PMMA (filled diamonds), and 40 wt % SAN2/60 wt % PMMA (filled hexagons). Curves in part b are fits to eq 3 with the parameters listed in Table 2.

The temperature dependence of the frequency-scale shift factors is shown in Figure 3b, along their apparent fits to eq 3 (solid curves). Plazek[45,50,51] has reported that the frequency-scale shift factors for PMMA cannot be described by eq 3 for data sufficiently close to T_g. While our PMMA shift factors fit the WLF equation reasonably (we are always more than 10 K above the DSC T_g), it is important to realize that such empirical relations are only approximate. Our WLF constants for the blends do not agree with those reported by Wu[37] ($C_1^g = 20.7$ and $T_\infty = T_g - 58$ K) for all SAN/PMMA blends (regardless of composition), from which we calculate $\alpha_f = 3.6 \times 10^{-4}$ K^{-1}. The fact that the coefficients of thermal expansion of the free volume in all of our SAN/PMMA blends are intermediate between those of the pure components, while Wu's α_f is a factor of 2 smaller, makes us suspect that something went wrong in Wu's analysis. Wu's PMMA has a different tacticity, and his SAN is a different composition, but it seems unlikely that such small microstructural differences could be sufficient to explain the large discrepancy noted.

The terminal relaxations of both SAN1 and PMMA are discernible in their blends, as shown in Figure 4. Comparison of the two sets of data allows us to conclude that the terminal (lowest frequency) relaxation corresponds to PMMA. This terminal relaxation manifests itself as a local maximum for the 20 wt % SAN1 blend and as a change in slope for the 30 wt % SAN1 blend. The SAN relaxation, at a higher frequency of roughly 2 rad/s, is less apparent in both blends, presumably due to the polydispersity and short chain length of SAN1 (see Table 1). The terminal relaxations of SAN2 and PMMA are too close to resolve cleanly.

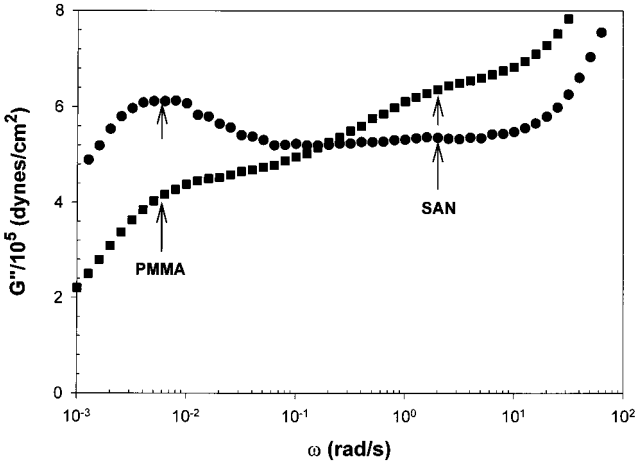

Figure 4. Loss modulus (G'') as a function of frequency (ω) for the 20 wt % SAN1/80 wt % PMMA blend at 184 °C = T_g + 64 K (circles) and the 30 wt % SAN1/70 wt % PMMA blend at 185 °C = T_g + 67 K (squares). The terminal relaxation times are 0.5 s for SAN1 and 200 s for PMMA.

Thermorheological simplicity has been observed in other blend systems characterized by dynamic symmetry. Friedrich *et al.*[15] have reported the results of oscillatory shear experiments on a blend of polystyrene/poly(cyclohexyl methacrylate) (PS/PCHM). This blend has a $\Delta T_g \cong 15$ K and $\Delta T_\infty \cong 40$ K. They have found that the tTS principle is approximately valid for the terminal relaxation in these blends. Alegria *et al.*[14] conclude that the dielectric α-relaxation is thermorheologically simple in miscible blends of poly(epichlorohydrin) and poly(vinyl methyl ether), for which $\Delta T_g = 0.8$ K and $\Delta T_\infty = 1$ K. These findings are convincing evidence that our results for SAN/PMMA are quite general for all blends with dynamic symmetry ($\Delta T_g \lesssim 30$ K). We next quantitatively test this generality using the temperature dependence of the minimum in tan δ as our quantitative measure of thermorheological complexity.

Our choice of tan δ arises from two observations that stem from the fact that tan δ is a ratio of moduli (see eq 2). For data analysis, tan δ is useful because modulus scale temperature shifts b_T do not affect tan δ, meaning that local extrema in tan δ do not change through tTS. More importantly, the accuracy of the tan δ measurement is much better than that of the measurement of moduli. Reproducibility in loading the sample typically results in ±5% errors in G' and G'', but the error in the measurement of the phase angle is much smaller, resulting in less than ±0.5% error for tan δ in the range $0.1 < \tan\delta < 10$. We focus on the minimum in tan δ at the high-frequency end of the rubbery plateau, simply because it is a convenient, well-defined point. The minimum, tan δ_{min}, is evaluated by fitting the tan δ data in the vicinity of the minimum to a cubic spline function of frequency. The temperature dependence of tan δ_{min} is plotted in Figure 5a for the pure components and the blends. We can typically evaluate tan δ_{min} over a 30−

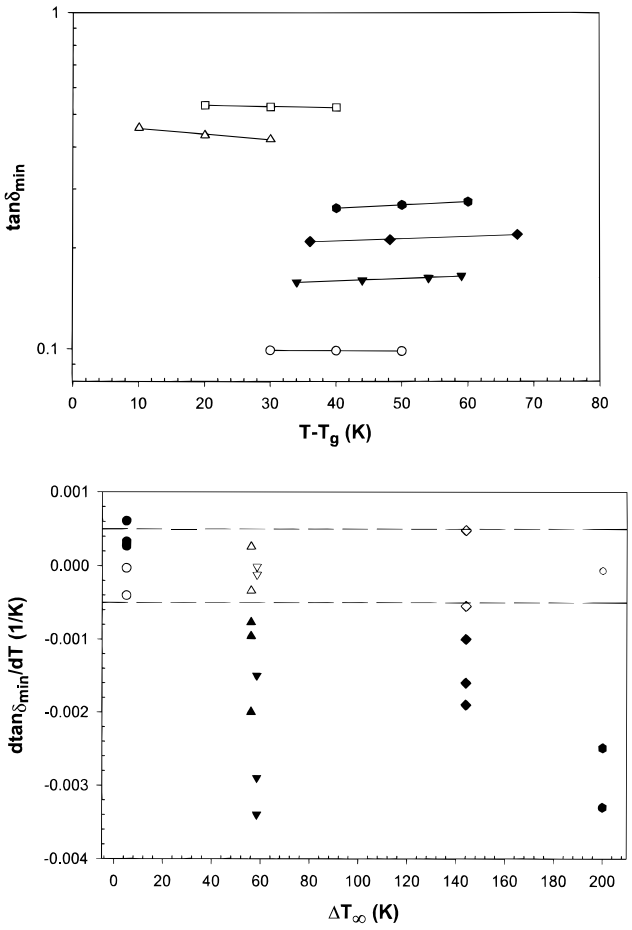

Figure 5. Quantitative measure of the quality of tTS. (a, top) Temperature dependence of the minimum in tan δ for SAN1 (open squares), SAN2 (open triangles), PMMA (open circles), and their blends: 20 wt % SAN1/80 wt % PMMA (inverted filled triangles), 30 wt % SAN1/70 wt % PMMA (filled diamonds), and 40 wt % SAN2/60 wt % PMMA (filled hexagons). (b, bottom) Change in the minimum of tan δ with changing temperature (d tan δ_{min}/dT) as a function of the difference in the Vogel temperatures of the pure components (ΔT_∞) for various miscible blends (filled symbols) and for their two pure components (open symbols): PMMA/SAN (circles), PI/PVE[7] (triangles), PB/PB[6] (inverted triangles), PS/PVME[52,53] (diamonds), and PEO/PMMA[4] (hexagons). The dashed horizontal lines in part b denote the limits expected for homopolymers.

40 K temperature range, and its value changes somewhat with temperature for both SAN and the blends. We use the temperature dependence of tan δ_{min} as a *quantitative measure of the failure of tTS*. Figure 5b shows d tan δ_{min}/dT as a function of the difference in Vogel temperatures of the pure components (ΔT_∞) for various miscible blends studied in the literature. For comparison, the values of this derivative determined for the two pure components of each blend are shown as open symbols in Figure 5b, at the same ΔT_∞ as that for the blend. All homopolymers shown exhibit some nonzero value of this derivative, indicating that tTS does not work perfectly, as has been reported previously.[45−47] However, the deviations from thermorheological simplicity are small for the homopolymers, as described by the following empirical result.

$$\left|\frac{\mathrm{d}\tan\delta_{min}}{\mathrm{d}T}\right| \lesssim 5 \times 10^{-4}\ \mathrm{K}^{-1}$$

The blends of SAN and PMMA show similar, very small departures from thermorheological simplicity, indicating that SAN/PMMA blends are nearly as thermorheologically simple as most homopolymers. In contrast, the mixed microstructure polybutadiene blends (PB/PB[6]) and blends of polyisoprene/polyvinylethylene (PI/PVE[7]), polystyrene/poly(vinyl methyl ether) (PS/PVME[52,53]), and poly(ethylene oxide)/poly(methyl methacrylate) (PEO/PMMA[4]) have values of the derivative that are considerably larger in magnitude than those for the corresponding homopolymers. PEO/PMMA shows a strong breakdown of the tTS and also has the largest Vogel temperature contrast (ΔT_∞). For a given blend system, the value of d tan δ_{min}/dT depends somewhat on the blend composition and the component molecular weights, but there does seem to be a trend of larger values of $-$d tan δ_{min}/dT for larger ΔT_∞. Thus it appears that the contrast in the Vogel temperatures of the components of a blend plays an important role in the thermorheological behavior.

V. Discussion

The observation of thermorheological complexity in miscible blends has been rationalized on the basis of a simple concentration fluctuation model.[16] We know from statistical mechanics that concentration fluctuations exist in any mixture. SANS measurements on polymer blends indicate that the fluctuations are sizable when the interactions between components are weak, and this is the basis for determining the Flory−Huggins interaction parameter χ from SANS. The scattering function (static structure factor) arising from concentration fluctuations in miscible blends is of the Ornstein−Zernike form[54] at low values of the isotropic scattering wave vector q.

$$S(q) = \frac{S(0)}{1 + q^2\xi^2} \tag{6}$$

The correlation length ξ for concentration fluctuations and the $q = 0$ limit of the scattering function $S(0)$ are related to χ in the random-phase approximation.[54]

$$\frac{\xi}{b} = \left(12\left[-2\chi\tilde{\phi}(1-\tilde{\phi}) + \frac{1}{N}\right]\right)^{-1/2} \tag{7}$$

$$S(0) = \left[-2\chi + \frac{1}{N\tilde{\phi}(1-\tilde{\phi})}\right]^{-1} = \frac{12\xi^2}{b^2}\tilde{\phi}(1-\tilde{\phi}) \tag{8}$$

The above equations are for a symmetric blend (with the same degree of polymerization N of each component). The monomer size (statistical segment length) is b, and the mean volume fraction of one component is $\tilde{\phi}$. Using the large N limit of eq 7 with a typical monomer size of $b = 6$ Å and a blend composition $\tilde{\phi} = 0.3$, and using the SANS determination[30−32] of $\chi = -0.01$, we estimate $\xi \cong 20$ Å for our SAN/PMMA blends. This correlation length is considerably smaller than those in two blend systems that show strong thermorheological complexity. The PI/PVE blends that exhibit thermorheological complexity have $\xi \cong 40$ Å. The PEO/PMMA blend that showed even stronger thermorheological complexity has $\xi \cong 100$ Å.[4] Even though SAN/PMMA blends have inherently smaller concentration fluctuations than either PI/PVE or PEO/PMMA, the fluctuations are sufficient to cause thermorheological complexity if the SAN/PMMA blend had large dynamic asymmetry. The time

scale for relaxation of these fluctuations is long,[55] so their presence can have a profound impact on chain dynamics.

The concentration fluctuations in miscible blends (measured by SANS) have a Gaussian distribution $P_{static}(\phi)$, centered about the mean blend composition $\tilde{\phi}$.

$$P_{static}(\phi) \sim \exp\left[\frac{-(\phi - \tilde{\phi})^2}{2\langle(\Delta\phi)^2\rangle}\right] \tag{9}$$

where

$$\langle(\Delta\phi)^2\rangle = \frac{b^3 S(0)}{V} = \frac{12\xi^2 b\tilde{\phi}(1-\tilde{\phi})}{V} \tag{10}$$

V is the volume over which the fluctuation is sampled. In SANS, V is a fixed scattering volume $\sim q^{-3}$, but for a dynamic probe the relevant volume is different. Here and elsewhere,[16] we rely on a phenomenological description of the glass transition. Segments in a small volume surrounding a given monomer are required to move cooperatively in order for the monomer to move.[56,57] The size of this cooperative volume V is a decreasing function of temperature and is believed to diverge at the Vogel temperature.[57]

$$V = \frac{(bd)^3 T_\infty^{\,2}}{(T - T_\infty)^2} \tag{11}$$

The parameter d is a material-specific dimensionless constant.[17] The size of the cooperative volume is clearly a function of local blend composition for blends of polymers with different T_∞'s. Regions rich in the low-T_∞ component have smaller cooperative volumes. Combining eqs 9−11, we see that, for a dynamic probe, the distribution of relevant concentration fluctuations is no longer symmetric about the mean blend composition.

$$P_{dynamic}(\phi) \sim \exp\left[\frac{-(\phi - \tilde{\phi})^2 b^2 d^3 T_\infty^{\,2}}{24\xi^2\tilde{\phi}(1-\tilde{\phi})\,(T - T_\infty)^2}\right] \tag{12}$$

As demonstrated previously,[16] eq 12 can have two local maxima, in some cases. One is centered on the mean blend composition ($\phi = \tilde{\phi}$), and the other corresponds to fluctuations that are rich in the low-T_g blend component (thereby maximizing $T - T_\infty$). The experimental evidence for two distinct compositions being seen by dynamic probes at the segmental level, while not overwhelming, is substantial, as discussed in detail elsewhere.[16] $P_{dynamic}(\phi)$ is converted into a predicted distribution of segmental relaxation times of each blend component using the WLF equation (eq 3), with appropriate truncations for chain connectivity effects.[16]

Many miscible blend pairs have relatively weak interaction between the components, and the components have different T_g's, for which the above considerations predict that tTS will fail. The concentration fluctuation model predicts that time−temperature superposition will be applicable only in the following three cases.

(1) In the case of *strong interactions* between components (making $\chi \ll 0$), concentration fluctuations are suppressed. $\xi \to 0$ in this case, and all cooperative volumes have precisely the same composition $\tilde{\phi}$. Thus, $P_{dynamic}(\phi) = \delta(\phi - \tilde{\phi})$, and the distribution of segmental relaxation times is unimodal. This limit is described by $V/(\xi^2 b) > 1$.

(2) When there is *dynamic symmetry*, the two components have closely-matched glass transition temperatures and Vogel temperatures. In this case all cooperative volumes are the same size and have identical dynamics (each has the same $T - T_\infty$), making $P_{dynamic}(\phi)$ a symmetric Gaussian function, for which tTS works, regardless of the magnitude of the fluctuations. Stated simply, each fluctuation has precisely the same local dynamics when there is no contrast in the glass transitions of the components of the blend.

(3) At sufficiently *high temperatures* ($T \gg T_\infty$) the cooperative volumes are all small, and the differences in their individual local dynamics diminish as temperature is raised. This is best seen in the Doolittle expression for the segmental relaxation time τ.

$$\tau \sim \exp\left(\frac{B}{\alpha_f(T - T_\infty)}\right) \tag{13}$$

As temperature is increased, the segmental relaxation time becomes progressively less sensitive to the Vogel temperature of a particular cooperative volume. Thus, as temperature is increased, tTS gradually becomes a better approximation, as long as the blend remains in a single-phase state.

The fact that SAN/PMMA blends comprise components with closely-matched glass transitions (see Table 2) means that the fluctuations in composition do not create regions with appreciably different local dynamics. Indeed, with the very small $\Delta T_\infty \leq 5$ K for SAN/PMMA blends, the concentration fluctuation model does not predict thermorheological complexity even if the correlation lengths were as large as 100 Å.[33]

The concentration fluctuation model predicts that tTS will fail only if the difference between the Vogel temperatures of the two components is sufficiently large. This prediction is demonstrated in Figure 6, where we plot the ratio of segmental relaxation times, predicted by the concentration fluctuation model, for a model blend of high molecular weight polymers with $\chi = 0$ (thereby having large concentration fluctuations) and identical WLF constants for both components ($C_1^g = 17.44$ and $C_2^g \equiv T_g - T_\infty = 51.6$ K[48]), but keeping ΔT_∞

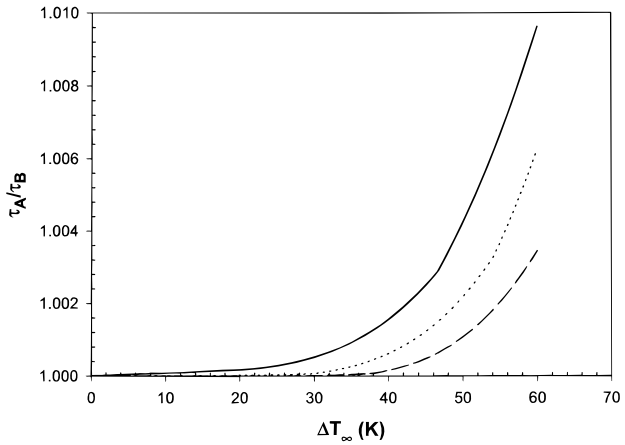

Figure 6. Dependence of the ratio of the segmental relaxation times of the components of a model binary miscible polymer blend with weak interactions ($\chi = 0$) on the difference between the Vogel temperatures of the components (ΔT_∞) for three temperatures: 420 K (solid curve), 430 K (dotted line), and 440 K (dashed curve). See text for details of the model.

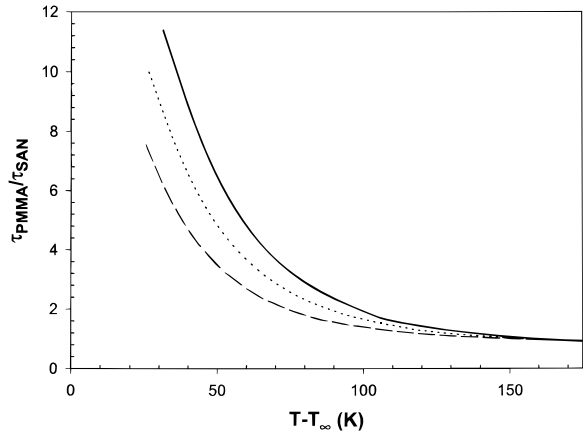

Figure 7. Temperature dependence of the ratio of the segmental relaxation times of SAN and PMMA, predicted by the concentration fluctuation model, and the Vogel temperature for various blends: 20 % SAN/80 % PMMA (solid curve), 30 % SAN/70 % PMMA (dotted curve), and 40% SAN/60 % PMMA (dashed curve).

as a free parameter. The glass transition of component A is 400 K, while the glass transition of component B is variable and below that of component A. Figure 6 shows that, in principle, blends with any dynamic asymmetry (*i.e.*, $\Delta T_\infty \neq 0$) should exhibit thermorheological complexity. However, in the temperature range covered by Figure 6, it would certainly be nearly impossible to observe thermorheological complexity in typical experiments if $\Delta T_\infty \lesssim 30$ K, while thermorheological complexity would be easily observed if ΔT_∞ were sufficiently large. Figure 6 also shows that the impact of concentration fluctuations on blend dynamics diminishes slowly as temperature is raised.

Figure 7 shows the dependence of the ratio of the segmental relaxation times of SAN and PMMA in a 20% SAN/80% PMMA blend, predicted by the concentration fluctuation model, as a function of the difference between the temperature and the blend Vogel temperature ($T - T_\infty$). For $T - T_\infty \gtrsim 80$ K, the ratio of segmental times is a weak function of temperature. This suggests that tTS should apply reasonably for SAN/PMMA blends at all temperatures above $T_\infty + 80$ K ($\cong T_g + 30$ K). However, complexity might be observed in SAN/PMMA blends closer to T_g. The superposition of tan δ for our blends in Figure 2 indeed suggests that the superposition is poorer at higher frequencies, where data were taken near T_g. The high-frequency maximum in tan δ, corresponding to the glass transition, shows quite poor superposition in Figure 2a and b. We typically need to be within ~30 K of T_g to see the high-frequency maximum in tan δ, so the stronger departure of these data from tTS is consistent with the expectations of the concentration fluctuation model. Figure 7 also shows the general trend that thermorheological complexity is more evident for blends rich in the high T_g component.

Our simple model of concentration fluctuations captures the role of ΔT_g in blend dynamics nicely. This model allows us to construct a "phase diagram" for miscible blends with weak energetic interactions that can be used to anticipate whether a blend will exhibit thermorheological complexity or not. Figure 8 shows the experimental ranges of the fractional free volume $f = \alpha_f(T - T_\infty)$, calculated assuming linear additivity of free volumes in blends, explored with oscillatory shear experiments for blends of different ΔT_g. We plot the

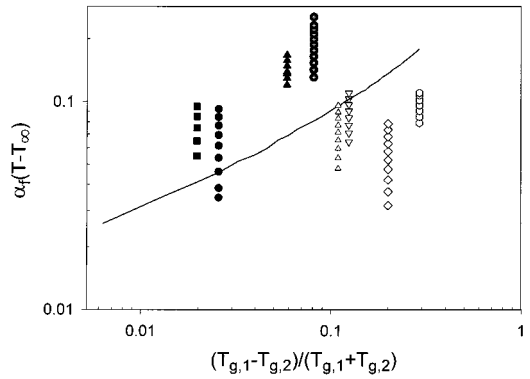

Figure 8. "Phase diagram" for weakly interacting miscible blends, correlating the thermorheological behavior in the parameter space of the free volume $\alpha_f(T - T_\infty)$ and the dimensionless dynamic asymmetry. All filled symbols denote blends which uphold tTS, and all open symbols denote blends for which tTS fails. The solid line is the theoretically predicted "phase boundary" which separates the regions where tTS works (at high temperatures and small ΔT_g) from those regions where it fails (at low temperatures and large (ΔT_g). The miscible blends are PS/PCHM[15] (filled squares), SAN/PMMA (filled circles), SAN/SMA[59] (filled triangles), hhPP/PEP[58] (filled circles with crosses), PB/PB[6] (open triangles), PI/PVE[7] (inverted open triangles), PS/PVME[52,53] (open diamonds), and PEO/PMMA[4] (open hexagons).

experimental measurement ranges of blends for which tTS is reported to apply as filled symbols (PS/PCHM,[15] SAN/PMMA, head-to-head polypropylene/polyethylenepropylene (hhPP/PEP[58]), and random SAN/alternating styrene−maleic anhydride copolymer (SAN/SMA[59])). The experimental ranges of mixed microstructure polybutadiene blends (PB/PB[6]) and PI/PVE,[7] PS/PVME,[52,53] and PEO/PMMA[4] blends, for which tTS fails, are plotted as open symbols.

To construct the phase boundary, we consider a series of hypothetical 50/50 blends with $\chi = 0$, for which each component has the same WLF coefficients[3] $C_1^g = 17.44$ and $C_2^g = T_g - T_\infty = 51.6$ K. The T_g of the low-T_g component is kept constant, while the T_g of the second component is varied. Since the cooperative volumes of various polymers are not known, we use our best estimates of these parameters determined for the PI/PVE system and thus assume that the low-T_g polymer has $d = 1.75$, while the high-T_g polymer has $d = 7.5$, with a simple linear mixing rule for the cooperative volume parameter d at intermediate compositions. For any real experiment, there will be a certain value of the slope in Figure 7 for which departures from thermorheological simplicity are discernible. In a general sense we write the criterion for thermorheological simplicity as a simple inequality.

$$\frac{d(\tau_A/\tau_b)}{dT} < a$$

τ_A and τ_B are the relaxation times of the low-T_g and high-T_g components, respectively. We evaluate the parameter $a = 0.05$ K^{-1} from the comparison with experimental data in Figure 8. The solid curve in Figure 8 is the model prediction with the parameters discussed above. Above and to the left of this curve, tTS is expected to work, while, below and to the right of this curve, tTS should fail. It is apparent from Figure 8 that blends with large dynamic asymmetry (large

ΔT_g) exhibit thermorheological complexity when they are studied sufficiently close to their glass transition temperatures. However, even for blends of PEO and PMMA, with $\Delta T_g = 180$ K, tTS is expected to work at temperatures exceeding 280 °C, but neither PEO nor PMMA are thermally stable at such high temperatures.

It is surprising how good a job our simple concentration fluctuation model does for separating regions of tTS applicability from regions of tTS failure. Clearly the phase boundary, drawn as the solid curve in Figure 8, should not be an abrupt boundary but rather a broad band where tTS nearly works as well as it does for homopolymer melts. We are in the process of better defining this boundary, in the hopes of transforming our correlative model into a predictive model.

VI. Conclusions

Blends of PMMA and SAN are characterized by dynamic symmetry, in that the glass transition temperatures of the pure components are closely-matched. Despite the fact that SANS experiments reveal the presence of significant composition fluctuations in this mixture, these fluctuations do not cause any measurable anomalous dynamics. The proximity of the Vogel temperatures of the pure components ($\Delta T_\infty \leq 5$ K) means that all composition fluctuations have similar Vogel temperatures, leading to thermorheological simplicity in these blends.

Using a simple model for the effects of concentration fluctuations on blend dynamics, we have rationalized the literature observations for the successes and failures of tTS in miscible blends. This resulted in a phase diagram for weakly interacting blends in the parameter space of free volume and ΔT_g that can be used to decide whether to expect tTS will work or not for a given blend.

Current work in our group on blends with dynamic symmetry is focusing on dynamics in blends of polyisobutylene and head-to-head polypropylene with $\Delta T_g = 30$ K. Other work on blends of polymers with sufficiently different Vogel temperatures (PS/PVME with $\Delta T_\infty \cong 140$ K, for example[53]) and also blends with very strong energetic interactions will be treated in forthcoming publications.

Acknowledgment. Financial support of this research from the National Science Foundation through Grant DMR-9629901 is acknowledged with gratitude. We thank Jacques E. L. Roovers for insightful comments on our manuscript and both Roovers and Marnix van Gurp for sharing their idea.

References and Notes

(1) Paul, D. R.; Newman, S. *Polymer Blends*; Academic Press: New York, 1978; Vol. 1.
(2) Utracki, L. A. *Polymer Alloys and Blends: Thermodynamics and Rheology*; Carl Hanser Verlag: Munich, 1990.
(3) Ferry, J. D. *Viscoelastic Properties of Polymers*, 3rd ed.; Wiley: New York, 1980.
(4) Colby, R. H. *Polymer* **1989**, *30*, 1275−1278.
(5) Roland, C. M.; Ngai, K. L. *Macromolecules* **1991**, *24*, 2261−2265.
(6) Roovers, J.; Toporowski, P. M. *Macromolecules* **1992**, *25*, 1096−1102.
(7) Roovers, J.; Toporowski, P. M. *Macromolecules* **1992**, *25*, 3454−3461.
(8) Chung, G. C.; Kornfield, J. A.; Smith, S. D. *Macromolecules* **1994**, *27*, 964−973.
(9) Chung, G. C.; Kornfield, J. A.; Smith, S. D. *Macromolecules* **1994**, *27*, 5729−5741.
(10) Arendt, B. H.; Kannan, R. M.; Zewail, M.; Kornfield, J. A.; Smith, S. D. *Rheol. Acta* **1994**, *33*, 322−336.
(11) Zawada, J. A.; Fuller, G. G.; Colby, R. H.; Fetters, L. J.; Roovers, J. *Macromolecules* **1994**, *27*, 6851−6860.
(12) Zawada, J. A.; Ylitalo, C. M.; Fuller, G. G.; Colby, R. H.; Long, T. E. *Macromolecules* **1994**, *27*, 6861−6870.
(13) Arendt, B. H.; Krishnamoorti, R.; Kornfield, J. A.; Smith, S. D. *Macromolecules* **1997**, *30*, 1127−1137.
(14) Alegria, A.; Elizetxea, C.; Cendoya, I.; Colmenero, J. *Macromolecules* **1995**, *28*, 8819−8823.
(15) Friedrich, C.; Schwarzwaelder, C.; Riemann, R. E. *Polymer* **1996**, *37*, 2499−2507.
(16) Kumar, S. K.; Colby, R. H.; Anastasiadis, S. H.; Fytas, G. *J. Chem. Phys.* **1996**, *105*, 3777−3788.
(17) Zetsche, A.; Fischer, E. W. *Acta Polym.* **1994**, *45*, 168−175.
(18) Stein, D. J.; Jung, R. H.; Ilers, K. H.; Sendus, H. *Angew. Makromol. Chem.* **1974**, *36*, 89−100.
(19) Naito, K.; Johnson, G. E.; Allara, D. L.; Kwei, T. K. *Macromolecules* **1978**, *11*, 1260−1265.
(20) McBrierty, V. J.; Douglass, D. C.; Kwei, T. K. *Macromolecules* **1978**, *11*, 1265−1267.
(21) Kressler, J.; Kammer, H. W.; Klostermann, K. *Polym. Bull.* **1986**, *15*, 113−119.
(22) Suess, M.; Kressler, J.; Kammer, H. W. *Polymer* **1987**, *28*, 957−960.
(23) Subramanian, R.; Huang, Y. S.; Roach, J. F.; Wiff, D. R. *Mater. Res. Soc. Symp. Proc.* **1990**, *171*, 217−224.
(24) Fowler, M. E.; Barlow, J. W.; Paul, D. R. *Polymer* **1987**, *28*, 1177−1184.
(25) Alegria, A.; Colmenero, J.; Ngai, K. L.; Roland, C. M. *Macromolecules* **1994**, *27*, 4486−4492.
(26) Song, M.; Hammiche, A.; Pollock, H. M.; Hourston, D. J.; Reading, M. *Polymer* **1995**, *36*, 3313−3316.
(27) Feng, H.; Ye, C.; Feng, Z. *Polym.* **1996**, *28*, 661−664.
(28) Pfennig, J. L. G.; Keskkula, H.; Barlow, J. W.; Paul, D. R. *Macromolecules* **1985**, *18*, 1937−1940.
(29) Brinke, G. T.; Karasz, F. E.; MacKnight, W. J. *Macromolecules* **1983**, *16*, 1827−1832.
(30) Jelenic, J.; Kirste, R. G.; Schmitt, B. J.; Schmitt-Strecker, S. *Makromol. Chem.* **1979**, *180*, 2057−2059.
(31) Schmitt, B. J.; Kirste, R. G.; Jelenic, J. *Makromol. Chem.* **1980**, *181*, 1655−1672.
(32) Hahn, K.; Schmitt, B. J.; Kirschey, M.; Kirste, R. G.; Salie, H.; Schmitt-Strecker, S. *Polymer* **1992**, *33*, 5150−5165.
(33) Kamath, S. Y.; Kumar, S. K.; Colby, R. H. Manuscript in preparation.
(34) Kim, E. Studies of Diffusion, Thermodynamics and Surface Segregation in Miscible Polymer Blends. Ph.D. thesis, Cornell University, Ithaca, NY, 1994.
(35) Kim, E.; Kramer, E. J.; Wu, W. C.; Garrett, P. D. *Polymer* **1994**, *35*, 5706−5715.
(36) Oultache, A. K.; Zhao, Y.; Jasse, B.; Monnerie, L. *Polymer* **1994**, *35*, 681−686.
(37) Wu, S. *Polymer* **1987**, *28*, 1144−1148.
(38) Wu, S. *J. Polym. Sci., Polym. Phys. Ed.* **1987**, *25*, 2511−2529.
(39) Han, C. D.; Kim, J. K. *Macromolecules* **1989**, *22*, 1914−1921.
(40) Han, C. D.; Kim, J. K. *Macromolecules* **1989**, *22*, 4292−4302.
(41) Yang, Y. H.; Han, C. D.; Kim, J. K. *Polymer* **1994**, *35*, 1503−1513.
(42) McMaster, L. P. *Adv. Chem. Ser.* **1975**, *142*, 43−70.
(43) Song, M.; Jiang, B. *Polymer* **1992**, *33*, 1445−1449.
(44) Higashida, N.; Kressler, J.; Inoue, T. *Polymer* **1995**, *36*, 2761−2764.
(45) Plazek, D. J. *J. Polym. Sci., Polym. Phys. Ed.* **1982**, *20*, 729−742.
(46) Plazek, D. J.; Rosner, M. J.; Plazek, D. L. *J. Polym. Sci., Polym. Phys. Ed.* **1988**, *26*, 473−489.
(47) Plazek, D. J.; Chay, I. C.; Ngai, K. L.; Roland, C. M. *Macromolecules* **1995**, *28*, 6432−6436.
(48) Williams, M. L.; Landel, R. F.; Ferry, J. D. *J. Am. Chem. Soc.* **1955**, *77*, 3701−3707.
(49) Vogel, H. *Phys. Z.* **1921**, *22*, 645−6.
(50) Plazek, D. J.; Tan, V.; O'Rourke, V. M. *Rheol. Acta* **1974**, *13*, 367−376.
(51) Plazek, D. J.; Raghupathi, N. *Polym. Prepr.* **1974**, *15*, 53−57.
(52) Pathak, J. A. Master's thesis, Penn State University, 1997.
(53) Pathak, J. A.; Colby, R. H.; Floudas, G.; Jerome, R. Submitted to *Macromolecules*.

(54) Doi, M. *Introduction to Polymer Physics*; Clarendon Press, Oxford, 1996.
(55) DeGennes, P. G. *J. Chem. Phys.* **1980**, *72*, 4756−4763.
(56) Matsuoka, S. *Relaxation phenomena in polymers*; Hanser: Munich, 1992.
(57) Donth, E. J. *Relaxation in Thermodynamics in Polymers*; Akademie Verlag: Berlin, 1992.
(58) Gell, C. B.; Krishnamoorti, R.; Kim, E.; Graessley, W. W.; Fetters, L. J. *Rheol. Acta* **1997**, *36*, 217−228.
(59) Van Gurp, M.; Palmen, J. *Rheol. Bull.* **1998**, *67*, 5−8.
(60) The force-rebalance transducer starts to exhibit compliance effects with 7.9 mm diameter plates at modulus levels exceeding 10^9 dyn/cm^2. Thus the data in Figures 1c and 2 at the highest frequencies are only qualitatively correct.

MA9805708